

Imino Proton Exchange and Base-Pair Kinetics in RNA Duplexes[†]

K. Snoussi and J.-L. Leroy*

*Laboratoire de Physique de la Matière Condensée, Groupe de Biophysique, UMR 7643 du CNRS, Ecole Polytechnique 91128 Palaiseau, France**Received February 23, 2001; Revised Manuscript Received April 27, 2001*

ABSTRACT: Using NMR magnetization transfer from water and ammonia-catalyzed exchange of the imino proton, we have measured the base-pair lifetimes and the dissociation constants of six RNA duplexes: [r(CGCGAUCGCG)]₂, [r(CGCGAAUUCGCG)]₂, [r(CCUUUCGAAAGG)]₂, [r(CGCACGUGCG)]₂, [r(GGU₈CC)•r(GGA₈CC)], and [poly(rA)•poly(rU)], and we compare them with those of their DNA homologues. As predicted by a two-state (closed/open) model of the pair, the imino proton exchange times decrease linearly vs. the inverse of catalyst concentration. As in DNA duplexes, base pairs open one at a time, and the kinetics is in most cases insensitive to the nature of the adjacent residues. The lifetime of the r(G•C) pairs, 40 to 50 ms, is longer than that of the equivalent in the corresponding oligodeoxynucleotides, and the dissociation constants, about 10⁻⁷, are slightly smaller. The r(A•U) opening and closing rates are much larger than those of the d(A•T) pairs, but the stabilities are comparable.

The H-bonded imino protons of nucleic acids are a probe of the base-pair opening-closing kinetics. Their exchange process for the Watson–Crick pairs is fairly well understood. It is interpreted by a two-state (closed/open) model of the pair (1). The imino protons are protected within the closed base pair (2). Exchange with water occurs from the transiently open pair via an acid–base reaction catalyzed by proton acceptors. The exchange rate may be limited either by the base-pair opening rate or by the imino proton-transfer rate. The base-pair lifetime is equal to the imino proton exchange time when the imino proton-transfer rate is not limiting, i.e., in the presence of a proton acceptor concentration such that exchange occurs at each opening event. When the proton acceptor concentration is limiting, the imino proton-transfer rate is reduced by comparison with that of the monomer by a factor equal to the apparent base-pair dissociation constant.

The base-pair kinetics has been characterized in B-DNA (3, 4) B'-DNA (5), and Z-DNA (6), in triple helices (7), in P-DNA (8), in an RNA–DNA hybrid (9), and in i-motif structures (10).

It is generally observed that the inner pairs of nucleic acid structures open one at a time. In B-DNA duplexes, their lifetimes range from 0.5 to 7 ms and 5 to 50 ms at 15 °C for the d(A•T) and d(G•C) pairs, respectively, and their dissociation constants from 10⁻⁵ to 10⁻⁷. The base-pair kinetics depends on the oligonucleotide structure. The d(A•T) lifetimes in the A-tracts of B'-DNA duplexes are in the range of 20 to hundreds of milliseconds at 15 °C (5, 11). Those of the d(G•C) pairs of Z-DNA duplexes are in the range of seconds (6).

Imino proton exchange times have been measured in several RNA structures (12, 13), but little is known about the RNA base-pair opening kinetics. The lifetimes of the r(A•U) and r(I•C) pairs of 50 base-pair long homopolymers are in the millisecond range at 15 °C (14). Lifetimes as long as minutes have been reported in transfer RNA for some base pairs of the D-stem region and of the T loop (15).

The determination of the base-pair lifetimes and dissociation constants provides an information complementary to the structural description of nucleic acids. In the context of a growing interest in RNA structures, we have undertaken an NMR¹ investigation of the imino proton exchange catalysis in RNA duplexes to collect a set of reference values of the lifetimes and dissociation constants of the RNA base pairs.

We have measured the imino proton exchange catalysis by ammonia and determined the base-pair lifetimes and dissociation constants of six RNA duplexes.

[r(CGCGAUCGCG)]₂, duplex I; [r(CGCGAAUUCGCG)]₂, duplex II and [r(CCUUUCGAAAGG)]₂, duplex III, were selected in view of the comparison with their DNA homologues whose base-pair lifetimes and dissociation constants were previously determined and which may be considered as benchmarks of proton exchange in DNA duplexes (1, 3, 4). [r(CGCACGUGCG)]₂, duplex IV, was studied in order to characterize the kinetics of an r(A•U) pair flanked on each side by a r(G•C) pair. [r(GGU₈CC)•r(GGA₈CC)], duplex V, was investigated to compare the r(A•U) and d(A•T) base-pair kinetics in the adenine tracts of RNA and DNA duplexes. To connect this study with an early investigation on imino proton exchange catalyzed by tris in [poly(rA)•poly(rU)],

[†] This work was supported in part by Grant 9272 (19 Décembre 1997) from the Association pour la Recherche contre le Cancer.

* Corresponding author: Fax: 33 1 6933 3004. E-mail: jll@pmc.polytechnique.fr.

¹ Abbreviations: DANTE, delays alternating with nutation for tailored excitation; JR, jump-and-return; NMR, nuclear magnetic resonance; NOESY, nuclear overhauser enhancement spectroscopy; EDTA, ethylene diamine tetraacetic acid.

duplex VI (13), we have measured the imino proton exchange catalysis by ammonia in the same 50 base-pair long duplex.

Furthermore, with the aim of evaluating the contribution of the methyl group to the difference observed between the d(A•T) and r(A•U) base-pair kinetics, we also measured imino proton exchange in [r(CGCGATCGCG)]₂ and [d(CGC-GAUCGCG)]₂, and we compared the exchange kinetics with those of [r(CGCGAUCGCG)]₂ and [d(CGCGATCGCG)]₂.

MATERIALS AND METHODS

Imino Proton Exchange Theory. The formalism of catalyzed proton exchange has been described (1, 16). The salient features relevant to this study are summarized below.

The imino proton exchange rate induced by a proton acceptor in an isolated nucleoside is

$$k_{\text{ex,acc}} = k_{\text{coll}}[\text{acc}]/(1 + 10^{\Delta pK})$$

where k_{coll} is the collision rate, [acc] is the proton acceptor concentration, and ΔpK is the pK difference between the imino proton and the acceptor.

Imino proton exchange from a base pair is a two-step process requiring base-pair opening, followed by transfer to a proton acceptor such as NH_3 . The proton acceptor contribution to the exchange time is given by

$$\tau_{\text{ex,cat}} = \tau_0 + 1/(k_{\text{ex,acc,open}}K_{\text{diss}}) \quad (1)$$

where τ_0 is the base-pair lifetime, K_{diss} the base-pair dissociation constant and $k_{\text{ex,acc,open}}$ the proton-transfer rate from the open pair.

A possible difference between the exchange rates of the isolated nucleoside and of the open pair is expressed by an accessibility factor, α , which should be equal to one in the case of perfect accessibility.

$$k_{\text{ex,acc,open}} = \alpha k_{\text{ex,acc}}$$

In DNA duplexes, the comparison of the exchange catalysis by proton acceptors of different sizes indicates a good accessibility of the imino proton in the open pair. Taking into account the small size and the neutral character of NH_3 , its accessibility factor may be considered close to one (17).

According to the two-state model, the plot of $\tau_{\text{ex,cat}}$ vs. the inverse of catalyst concentration is a straight line whose extrapolation to infinite catalyst concentration yields the base-pair lifetime τ_0 . The apparent dissociation constants, αK_{diss} , were computed according to expression 1 from the ratio of the rates of exchange catalysis measured in the duplex and for the isolated nucleoside (17). The apparent lifetime of the open pair, $\alpha\tau_{\text{open}}$, is equal to the product $\tau_0\alpha K_{\text{diss}}$.

In the absence of added catalyst, exchange is due to a concerted transfer involving one or several water molecules bridging the imino proton of the open pair and the cyclic nitrogen of the complementary base [C (N3) in the case of a (G•C) pairs and A (N1) for an (A•U) pairs] which acts as an intrinsic catalyst (18). The imino proton exchange rate induced by this process depends on the difference, ΔpK , between the imino proton and the cyclic nitrogen pK of the complementary base pair:

$$k_{\text{ex,aac}} = k_{\text{ex,open}}^{\text{int}} K_{\text{diss}} 10^{(1+\Delta pK)}$$

The concerted transfer rate $k_{\text{ex,open}}^{\text{int}}$ is in the range of 10^{-6} in the case of B-DNA duplexes.

Intrinsic catalysis may be significant at neutral or acid pH. At high pH, hydroxyl catalysis takes over.

Oligonucleotide Synthesis. The oligoribonucleotides were synthesized on a 2 μM scale with a Pharmacia gene assembler using phenoxyacetyl β -cyanoethyl phosphoramidites as previously described (19). They were purified on a Q sepharose Hiload column using a NaCl gradient in a urea, 4 M solution, buffered at pH 7 by phosphate, 5 mM. After purification, they were then dialyzed against a 5 mM NaCl solution and finally against water. The preparation and purification of [poly(rA)•poly(rU)] have been already described (14). Concentrations of nucleic acid duplexes were determined from the absorbance at 260 nm using the A^{260} values computed according to a nearest neighbor model (20). The DNA sequence d(CGCGAUCGCG) was synthesized on a 2 μM scale and purified as previously described (1).

Sample Preparation. The oligonucleotides were dissolved at the strand concentration of 0.5 to 1.5 mM in 400 μL of a 90% H_2O , 10% D_2O solution containing 0.1 M NaCl, 1 mM EDTA, and 0.2 mM of 2,2-dimethyl-2-silapentane-5-sulfonate, whose methyl peak was set to 0 ppm for chemical shift reference. The pH was adjusted using 0.1 to 1 M HCl and NaOH solutions and measured at room temperature before and after each experiment. The samples were rapidly vortexed after addition of NaOH to avoid degradation by a strong local OH^- concentration. They were kept under nitrogen atmosphere in the NMR tube. The absence of phosphomonoester and of 2'-3' cyclic phosphate peaks in the ^{31}P NMR spectra is a good indicator of sample integrity.

The catalysts were added to the samples from stock solutions, whose concentrations ranged from 1 M for phosphate to 6.5 M for ammonia.

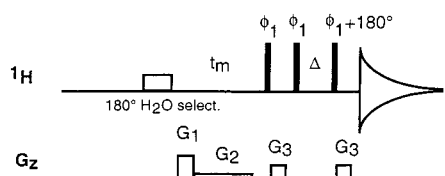
Unless otherwise stated, ammonia-catalyzed exchange was measured at pH 8.9, a value high enough to provide a fair proportion of NH_3 but low enough to avoid strong catalysis by OH^- .

NMR Methods. Imino proton exchange times were measured by 1D NMR methods using a 500 MHz Varian Unity INOVA spectrometer. The imino protons were assigned by 2D NOESY spectra collected with mixing times of 70 and 300 ms.

Exchange times longer than 5 ms were obtained by magnetization transfer from water as previously reported (1) using the sequence described in Scheme 1. The water magnetization was inverted by a DANTE sequence (21) of 30 hard 6° pulses separated by 50 μs intervals. The small water residual transverse component due to pulse imperfections was destroyed by a 23 G/cm 0.5 ms Z-gradient (G1) applied after the DANTE sequence. A 0.01 G/cm Z-gradient (G2) was applied during the magnetization transfer delay. The signal was detected according to Scheme 1 (22) using an echo water suppression subsequence. The exchange contribution of the added catalyst was determined from the exchange times measured in the presence (τ_{ex}) and in the absence (τ_{ex0}) of catalyst by

$$\tau_{\text{ex,cat}} = (1/\tau_{\text{ex}} - 1/\tau_{\text{ex0}})^{-1}$$

The exchange times were computed from the imino proton magnetization measured after 16 to 24 t_m increments (1).

Scheme 1: Pulse Sequence for Magnetization Transfer and Proton Exchange Measurements^a

^a First line: ¹H RF pulses. The pulse phases are indicated. The open rectangle represents the DANTE sequence which selectively inverts the water magnetization. The filled rectangles represent 90° hard pulses. Second line: gradient pulses. G1 and G2 gradients reduce radiation damping after water inversion. The signal is detected with a symmetrical echo water suppression subsequence, which therefore contributes to the amplitude but not to the phase of the frequency response. In the present case, the amplitude response goes as sin squared of the frequency offset from water. The magnetization is spread out by the first G3 gradient pulse (15 G/cm during 0.3 ms). The Δ delay was set to 115 μs, the time allowing the 180° precession of the imino proton which is required for optimal refocussing of the imino proton isochromates

Spurious effects due to cross-relaxation were limited by using mixing times shorter than 150 ms. The absence or the weakness of cross-relaxation effects was controlled by following the magnetization of the adenosine H2 protons which are close to the fast exchanging A•U imino protons.

The exchange times shorter than 5 ms were determined from the imino proton line broadening induced by the catalyst or from the longitudinal relaxation times in the presence (T_1) and in the absence of added catalyst (T_{10}). In that case, the exchange contribution of the added catalyst was computed as:

$$\tau_{\text{ex,cat}} = (1/T_1 - 1/T_{10})^{-1}$$

In these experiments, the imino proton magnetization was inverted by a DANTE sequence as previously described (1) and detected by the JR excitation sequence (23) after a variable delay. Thirty variable delays were used to compute each relaxation time.

RESULTS AND DISCUSSION

Imino Proton Exchange versus pH in [r(CGCGAUCGCG)]₂. The imino proton exchange times of [r(CGCGAUCGCG)]₂ are displayed in the absence of NH₃ or other

proton acceptor vs. pH in Figure 1. The comparison with the exchange times of the homologous DNA duplex (24) shows that imino proton exchange is controlled by the same processes in the oligoribo- and oligodeoxynucleotide duplexes.

At high pH, the straight lines with a -1 slope indicate catalysis by OH⁻. The rate of hydroxyl catalysis is slowed by comparison with that of the monomer by a factor corresponding to the apparent base-pair dissociation constant αK_{diss} . The pH-independent exchange process observed around pH 7.5 for the G imino protons and between pH 8 and pH 5 for the U imino proton is assigned to the intrinsic catalysis by the nitrogen of the complementary base (18). The acid-induced exchange of the (G•C) imino protons has been ascribed to the same process, but exchange occurs in that case from the pH-dependent fraction of N7-protonated guanosine, whose imino proton exchanges more rapidly because of its lower pK (25).

The similarity of the intrinsic catalysis rates measured in the RNA and DNA duplexes suggests an open state structure of the RNA pairs in which one or several water molecules bridge the imino proton and the cyclic nitrogen of the complementary base.

Base-Pair Dissociation Constant in [r(CGCGAUCGCG)]₂. We have measured the effects of phosphate (pK = 6.8), imidazole (pK = 6.95), triethanolamine (pK = 7.72), tris (pK = 8.08), and glycine (pK = 9.8) on the exchange times of the four inner imino protons of [r(CGCGAUCGCG)]₂ at 25 °C. Exchange catalysis was measured 0.3 pH units above the proton acceptor pK, except for glycine where pH was 9.6. To assess a possible destabilization of the pairs induced by deprotonation of the C2'-OH (pK ≈ 12) (26) at high pH, the exchange catalysis by ammonia was measured at both pH 8.9 and 9.9.

The apparent dissociation constants αK_{diss} for each catalyst are displayed in Figure 2.

The similarity of the dissociation constants derived from the exchange catalysis by ammonia at pH 8.9 and 9.9 shows that the base-pair dissociation constant is not pH-dependent.

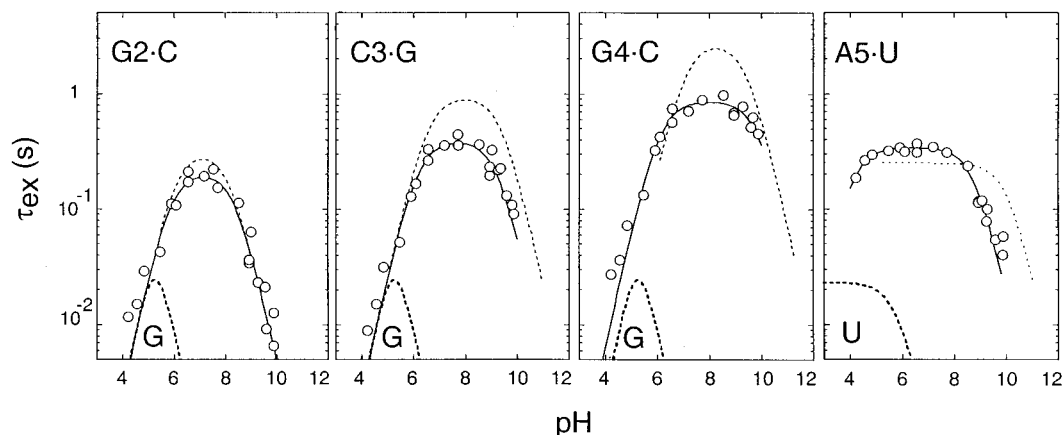


FIGURE 1: Imino proton exchange times versus pH in the [r(CGCGAUCGCG)]₂ duplex at 25 °C. The data are analyzed in terms of three exchange processes. The imino proton exchange times in the DNA homologous sequence (24) are also displayed for comparison (thin dotted lines). At high pH, the straight line with a negative slope is characteristic of catalysis by OH⁻. It is displaced vertically from the line corresponding to the monomer (heavy dotted lines) by a factor equal to αK_{diss} , the apparent dissociation constant. The pH-independent exchange process observed between pH 7 and 9 for the G imino protons and below pH 8 for the U imino proton, is due to intrinsic catalysis. Below pH 7, the acid-induced exchange of the G imino protons is due to intrinsic catalysis occurring from N7-protonated guanosine.

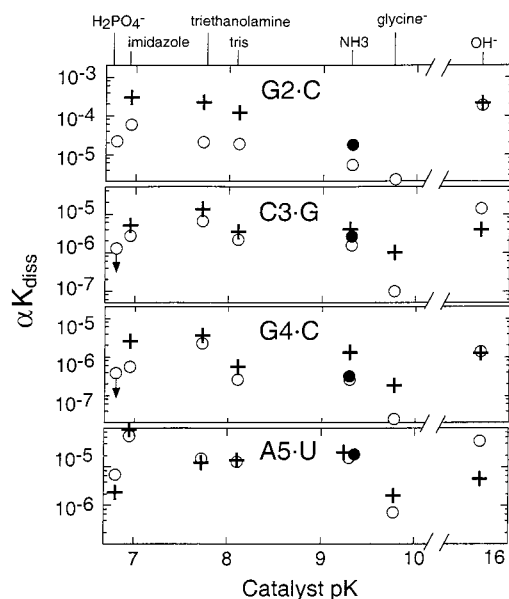


FIGURE 2: Apparent dissociation constant of the $[r(\text{CGC-GAUCGCG})]_2$ base pairs at 25 °C, derived from imino proton exchange catalysis by phosphate ($\text{pK} = 6.8$), imidazole ($\text{pK} = 6.95$), triethanolamine ($\text{pK} = 7.72$), tris ($\text{pK} = 8.08$), ammonia ($\text{pK} = 9.25$) at pH 8.9, glycine ($\text{pK} = 9.8$), and OH^- ($\text{pK} = 15.7$) (\circ). The apparent dissociation constants derived from the ammonia catalysis at pH 9.9 (\bullet). Apparent base-pair dissociation constants determined with the same catalyst in the DNA homologous sequence $[d(\text{CGCGATCGCG})]_2$ are indicated (+) for comparison (replotted from ref 17). The arrows indicate that the data points are upper limits. The dissociation constants of RNA and DNA pairs are quite close, except for G2·C. The smaller αK_{diss} values measured for r(G2·C) indicates a reduction of the end-fraying propagation in the RNA duplexes.

For a given base pair, the αK_{diss} values derived for all catalysts, except glycine, are in good agreement with a dispersion smaller than a factor of 10, as in the case of the DNA homologues. The dispersion may be due to differences of the imino proton accessibility for the catalysts in the open pair. The similarity of the RNA base-pair dissociation constants determined with small (NH_3), bulky (tris), neutral and negatively charged proton acceptors indicates that the access to the imino proton of the open pair is not hindered by a steric or an electrostatic barrier. Thus, as in the case of the DNA oligonucleotides, the α factor may be assumed close to one.

The apparent dissociation constants of corresponding r(A·U) and d(A·T) pairs in homologous RNA and DNA duplexes are comparable. The values for r(G·C) are somewhat smaller than those of their DNA counterparts.

The smaller apparent dissociation constants derived in the case of glycine corresponds to a weaker efficiency of this catalyst for exchange of the imino proton in the open pair. This unexplained property applies to both RNA and DNA.

Ammonia-Catalyzed Imino Proton Exchange. The ammonia contribution to imino proton exchange in $[r(\text{CGC-GAUCGCG})]_2$ displayed in Figure 3 is typical of the exchange measurements performed in the other oligoribonucleotides.

As with DNA duplexes, the imino proton of the outer pair is broadened out by hydroxyl catalysis at pH 8.9, 15 °C. The linear dependence of $\tau_{\text{ex},\text{NH}_3}$ vs the inverse of the ammonia concentration is consistent with an exchange process occurring from a single open state. The base-pair

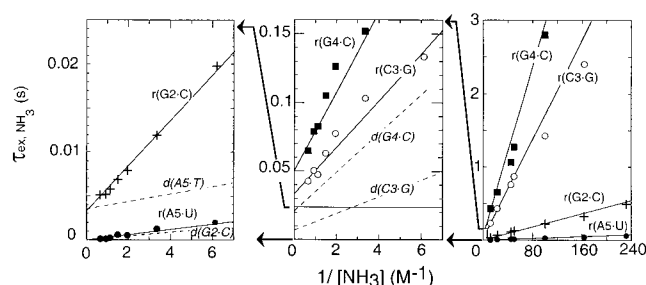


FIGURE 3: Ammonia contribution to the exchange time of the imino protons of $[r(\text{CGCGAUCGCG})]_2$. G2·C ($+$), C3·G (\circ), G4·C (\blacksquare), and A5·U (\bullet). The ammonia contribution to the exchange time vs the inverse of the NH_3 concentration is a straight line. Extrapolation to infinite catalyst concentration yields the base-pair lifetime. The lower left corner of the right panel is enlarged in the central panel. The left panel shows the extrapolation at high ammonia concentration of the exchange times of G2·C and A5·U imino protons. The dashed lines show the ammonia contribution to imino protons exchange in the homologous DNA duplex (3). Solution conditions: NaCl 0.1 M, pH 8.9, $T = 15$ °C.

lifetimes obtained by extrapolation of the NH_3 exchange contribution to infinite ammonia concentration are: 3.4, 33, and 50.6 ms, respectively, for r(G2·C), r(C3·G), and r(G4·C). The exchange time of the r(A5·U) imino proton extrapolates to a value too short to be measured, indicating a base-pair lifetime shorter than 0.1 ms. Its lifetime at 0 °C, 1 ms, is about 10 times shorter than that of the d(A·T) pair of the homologous sequence.

The base-pair lifetimes, τ_0 , and the apparent dissociation constants αK_{diss} of the six oligoribonucleotides studied are listed in Table 1, together with the base-pair opening activation energies obtained from the van't Hoff plot of the base-pair lifetimes measured at 0, 5, 15, 25, and 35 °C. The open pair lifetimes (i.e., the products $\tau_0 \alpha K_{\text{diss}}$) are also tabulated.

Effect of U/T Substitution in RNA and DNA Duplexes. To distinguish between effects of the change from ribo to deoxyribo (e.g., from B-DNA to A-RNA) and from T to U, we compared imino proton exchange in four species, namely, duplex I both ribo and deoxy, and in two duplexes derived from them by substitution of rT for rU and of dU for dT.

The base-pair lifetimes, the dissociation constants, and the open state lifetimes displayed in Figure 4 show that the difference between the d(A·T) and the d(A·U) base-pair kinetics is not related to the methyl group. In $[r(\text{CGC-GAUCGCG})]_2$ and $[r(\text{CGCGATCGCG})]_2$, both r(A·U) and r(A·T) lifetimes are shorter than 0.1 ms. In the oligodeoxynucleotides, the lifetime of the d(A·U) pair, 1.2 ± 0.5 ms, is shorter than that of d(A·T), 3.5 ± 0.5 ms, but it remains at least 10 times longer than that of the r(A·U/T) pairs of the RNA duplexes. It may be noted that the lack of marked effects of the methyl group on the A·U/T base-pair kinetics is consistent with the similarity of the d(G·C) and d(G·5mC) base-pair lifetimes in DNA duplexes (3).

It is remarkable that the kinetics of the (G·C) pair flanking the (A·U/T) pair is affected by the U/T substitution. In the RNA duplex, the lifetime of the r(G4·C) pair adjacent to the r(A·U) pair, 50.6 ms, increases to 77 ms by substitution of T for U. In the DNA duplex, the lifetime of d(G4·C) is not affected when dT is replaced by dU, but the dissociation constant of this pair increases by a factor of 3. This indicates either a longer open pair lifetime of the d(G·C) pair adjacent

Table 1: Lifetimes τ_0 ; Base-pair Opening Activation Energies, E_a ; Apparent Dissociation Constants, αK_{diss} , and Apparent Open Pair Lifetimes $\alpha\tau_{\text{open}}$ in RNA Duplexes at 15 °C^a

sequences	number	base pairs				
r(CGCGAUCGCG)	I	G2•C	C3•G	G4•C	A5•U	
τ_0 (ms)		3.4 ($\ll 1$)	33 (7)	50.6 (21.5)	≤ 0.1 (3.5)	
E_a (kJ/mol)		68	110 (47)	66 (46)	75 (42)	
r(CGCGAAUUCGCG)	II	G2•C	C3•G	G4•C	A5•U	A6•U
τ_0 (ms)		4.8 ($\ll 1$)	39 (4)	55 (25)	≤ 0.1 (8)	0.4 (30)
E_a (kJ/mol)		78	98	51		
r(CCUUUCGAAAGG)	III	C2•G	U3•A	U4•A	U5•A	C6•G
τ_0 (ms)		2.2 ($\ll 1$)	≤ 0.1 (3.5)	≤ 0.1 (6.5)	0.32 (4)	52.8 (40)
E_a (kJ/mol)		85	46 (43)	51.5 (52)	66 (65)	65 (65)
r(CGCACGUGCG)	IV	G2•C	C3•G	A4•U	C5•G	
τ_0 (ms)		4.7	26	1.8	42	
E_a (kJ/mol)		75	80	58	55	
r(GGUUUUUUUUCC)	V	G2•C	U3•A	U4–9•A ^b	U10•A	C11•G
τ_0 (ms)		5	1.7	2.3	0.7	11
E_a (kJ/mol)		73		42		
[poly(rA)•poly(rU)]	VI					
τ_0 (ms)		3				
E_a (kJ/mol)		71 ^b				
r(CGCGAUCGCG)	I	G2•C	C3•G	G4•C	A5•U	
$\alpha K_{\text{diss}} \times 10^6$		2.2 (20)	0.28 (0.57)	0.16 (0.26)	8.2 (4.5)	
r(CGCGAAUUCGCG)	II	G2•C	C3•G	G4•C	A5•U	A6•U
$\alpha K_{\text{diss}} \times 10^6$		0.85	0.12 (0.56)	0.1 (0.17)	13.4 (4.5)	3.2 (2)
r(CCUUUCGAAAGG)	III	C2•G	U3•A	U4•A	U5•A	C6•G
$\alpha K_{\text{diss}} \times 10^6$		1.9	14 (30)	4.4 (17)	3.5 (15)	0.18 (0.3)
r(CGCACGUGCG)	IV	G2•C	C3•G	A4•U	C5•G	
$\alpha K_{\text{diss}} \times 10^6$		1.5	0.07	2.48	0.11	
r(GGUUUUUUUUCC)	V	G2•C	U3•A	U4–9•A ^c	U10•A	C11•G
$\alpha K_{\text{diss}} \times 10^6$		16.5	18.5	17	49	20.8
[poly(rA)•poly(rU)]	VI					
$\alpha K_{\text{diss}} \times 10^6$		46.6				
r(CGCGAUCGCG)	I	G2•C	C3•G	G4•C	A5•U	
$\alpha\tau_{\text{open}}$ (ns)		7.5 ($\ll 20$)	9.2 (4)	8.1 (5.6)	≤ 0.8 (15.7)	
r(CGCGAAUUCGCG)	II	G2•C	C3•G	G4•C	A5•U	A6•U
$\alpha\tau_{\text{open}}$ (ns)		4.1	4.7 (2.2)	5.5 (4.2)	≤ 1.3 (36)	1.3 (60)
r(CCUUUCGAAAGG)	III	C2•G	U3•A	U4•A	U5•A	C6•G
$\alpha\tau_{\text{open}}$ (ns)		4.2	≤ 1.4 (105)	≤ 0.4 (110)	1.1 (60)	9.5 (12)
r(CGCACGUGCG)	IV	G2•C	C3•G	A4•U	C5•G	
$\alpha\tau_{\text{open}}$ (ns)		7	1.8	4.5	4.6	
r(GGUUUUUUUUCC)	V	G2•C	U3•A	U4–9•A ^c	U10•A	C11•G
$\alpha\tau_{\text{open}}$ (ns)		82.5	31.4	39.1	34.3	229
[poly(rA)•poly(rU)]	VI					
$\alpha\tau_{\text{open}}$ (ns)		140				

^a The parameters measured in the equivalent DNA oligonucleotides are given inside parentheses. The uncertainties on base-pair lifetimes are estimated as $\pm 20\%$ for the longer values and $\pm 50\%$ for the smaller values. The uncertainties on dissociation constants are about $\pm 15\%$. ^b From ref 14. ^c Nonresolved imino proton peak.

to the d(A•T) or an increased accessibility of its imino proton. As expected, the U/T substitution has little or no effect on the kinetics of the (G2•C) and (C3•G) pairs.

Base-Pair Kinetics in RNA Duplexes. Several differences emerge from the comparison of the base-pair kinetics and stability in RNA and DNA duplexes (Figure 5).

(a) *Kinetics of the A•U Pairs.* The r(A•U) base-pair lifetimes are much shorter than those of the d(A•T) pairs of the homologous DNA sequences. The single exception is for the r(A•U) pair flanked on each side by a r(G•C) pair in duplex IV, whose lifetime, 1.8 ms at 15 °C, is typical of the values found for the d(A•T) pairs in B-DNA duplexes. In duplexes I, II, and III, the exchange times of most of the r(A•U) imino protons extrapolate at infinite ammonia

concentration to values shorter than 0.1 ms at 15 °C. In accordance with an early investigation of imino proton exchange catalyzed by tris in [poly(rA)•poly(rU)] (14), the exchange catalysis by ammonia indicates base-pair lifetimes in the range of 2 to 3 ms for the r(A•U) pairs in the long rA-tracts of [poly(rA)•poly(rU)] and duplex V (Table 1).

The apparent dissociation constants of the r(A•U) fall in the same range of values as those of d(A•T) pairs of B- and B'-DNA duplexes: 2×10^{-6} to 5×10^{-5} at 15 °C (Figure 5). This indicates that the lifetimes of the open and closed r(A•U) pairs are reduced in comparable proportion with those of the d(A•T). By contrast with the lifetimes of the open d(A•T) pairs in B'- and B-DNA duplexes, which fall in a rather narrow range of values, the lifetimes of the open r(A•

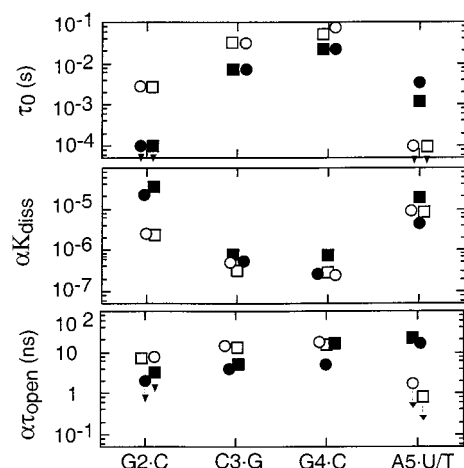


FIGURE 4: U/T substitution effect on the base-pair lifetimes, apparent dissociation constants and open pair apparent lifetimes in RNA and DNA homologous duplexes. $[\text{r}(\text{CGCGAUCGCG})]_2$ (\square); $[\text{r}(\text{CGCGATCGCG})]_2$ (\circ); and in duplexes $[\text{d}(\text{CGCGAUCGCG})]_2$ (\blacksquare) and of $[\text{d}(\text{CGCGATCGCG})]_2$ (\bullet). The parameters related to the latter deoxy-duplex are replotted from refs 3 and 30. The arrows indicate that the data points are upper limits. Solution conditions: NaCl 0.1 M, pH 8.9, $T = 15^\circ\text{C}$.

U) pairs in the RNA duplexes are scattered over 3 orders of magnitude.

(b) *Kinetics of G·C Pairs.* The lifetimes and the dissociation constants of the inner $\text{r}(\text{G}\cdot\text{C})$ pairs fall within a narrow range of values. Their lifetimes, 26 to 55 ms, are at the upper limit of those of the $\text{d}(\text{G}\cdot\text{C})$ pairs, and their apparent dissociation constants are slightly smaller (Table 1 and Figure 5). The lifetimes of the open $\text{r}(\text{G}\cdot\text{C})$ pairs are in the range of 1.8 to 9.5 ns.

Activation Energy. The opening activation energies of the $\text{r}(\text{G}\cdot\text{C})$ and $\text{r}(\text{A}\cdot\text{T})$ pairs, 51 to 110 kJ/mol and 46 to 75 kJ/mol, respectively, are comparable or slightly larger than those of the DNA duplexes (3, 4, 11). The $\tau_0\alpha K_{\text{diss}}$ products, i.e., the estimated τ_{open} , are nearly independent of the temperature between 0 and 35°C (not shown), indicating a weak closing activation energy.

Fraying of the RNA Duplexes. As in DNA duplexes, the lifetime of the outermost G·C pair is too short to be measured

at 15°C . The lifetime of the second pair is in the range of 2 to 5 ms, as compared to less than 1 ms in the DNA duplexes. In duplex I, the apparent dissociation constant of G2·C, which is about 10 times smaller than that of the corresponding pair of the homologous DNA duplex, indicates a reduced end-fraying propagation. This feature could be related to increased sugar rigidity caused by the $(\text{C}-\text{H}2')_n \cdot (\text{O}4')_{n+1}$ bonds reported for the RNA helix, or by H-bonding of C2'-OH to a sugar oxygen or to a minor groove atom of its own base (27).

Concluding Remarks. Imino proton exchange catalysis is basically similar in RNA and DNA duplexes. The linearity of the added catalyst contribution to the exchange time vs the inverse of the catalyst concentration shows that imino proton exchange may be interpreted by a two-state (closed/open) model. It is noteworthy that the nonlinearity of the exchange contribution of NH_3 recently reported in a proton exchange study of $[\text{d}(\text{CGCGAATTCGCG})]_2$ and of $[\text{d}(\text{CGCA}_8\text{CGC})\cdot\text{d}(\text{GCGU}_8\text{GCG})]$ (11) is not observed in the case of their RNA homologues (duplexes II and V). The RNA base pairs open independently of each other, and their lifetimes are not directly related to the nature of the adjacent pairs. The base-pair opening activation energies obtained for duplex III are nearly the same as those found for the DNA homologous sequence. Nevertheless, the opening activation energies of the RNA base-pairs are on average about 40% larger than those found for the B-DNA base pairs.

The intrinsic catalysis rates and the imino proton accessibility in the open RNA and DNA base pairs argue for comparable opening amplitudes in the oligoribo- and oligodeoxynucleotides. It may be noted that the proton exchange experiments do not indicate the opening amplitude reduction predicted by a recent comparative calculation of the base-pair opening in RNA and DNA duplexes (28).

The most conspicuous differences between the RNA and the DNA base-pair kinetics are the fast opening-closing rate of the $\text{r}(\text{A}\cdot\text{U})$ pairs, the enhanced stability, and the long lifetime of the $\text{r}(\text{G}\cdot\text{C})$ pairs.

Examination of Figure 5 shows that the opening-closing kinetics of the $\text{r}(\text{A}\cdot\text{U})$ pairs of $[\text{poly}(\text{rA})\cdot\text{poly}(\text{rU})]$ and of

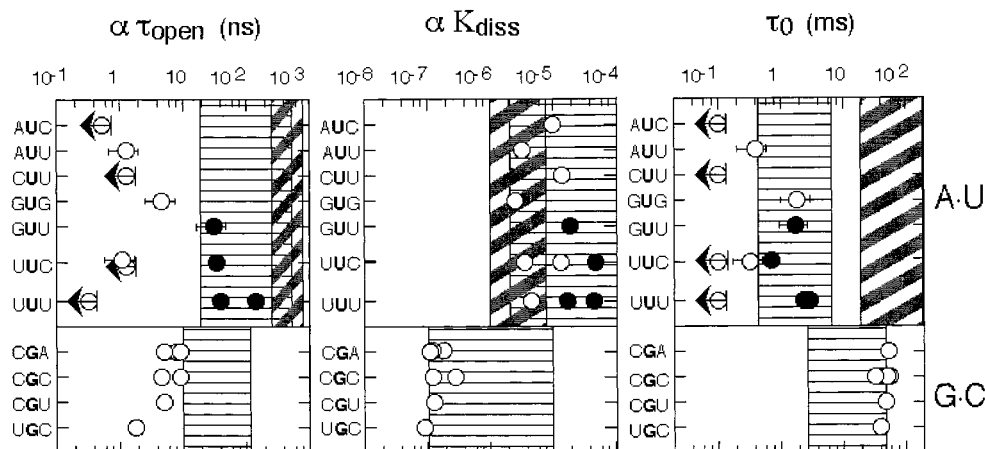


FIGURE 5: Base-pair lifetimes, apparent dissociation constants, and apparent open pair lifetimes in RNA duplexes at 15°C . The parameters related to the $\text{r}(\text{A}\cdot\text{U})$ pairs of the rA-tracts in $[\text{poly}(\text{rA})\cdot\text{poly}(\text{rU})]$ and of sequence V are indicated by filled circles. The values correspond to the central base pair of the specified 5'-3' triplet. The arrows indicate that the data points are upper limits. Representative error bars are displayed for some A·U base-pair lifetimes. The error bars on the dissociation constants and on the G·C base-pair lifetimes are smaller than the size of the data points. The vertically and the diagonally stippled areas show respectively the ranges of values determined for the B-DNA base pairs (24) and for the $\text{d}(\text{A}\cdot\text{T})$ pairs in the dA-tracts of B'-DNA structures (5, 11, 17).

duplex V is significantly slower than that of the r(A•U) pairs of the other duplexes. This suggests that the long r(A)•r(U) sequences could form a distinct conformational class.

The comparison of the DNA and RNA duplexes stabilities has been the subject of numerous studies. The melting temperature of the RNA duplexes is generally higher than that of the DNA homologues. The single exception is for long rA-tracts duplexes, whose melting temperature is close to or even lower than that of their homologous B'-DNA duplexes. A study carried out on 14 homologous RNA and DNA duplexes of 8 to 21 residues shows that the excess of free energy for the RNA duplexes is about 3 kJ/mol per r(G•C) pair and less than 0.4 kJ/mol per r(A•U) pair (29). This indicates that the dissociation constants of the r(G•C) pairs are reduced by a factor $\exp(3000/RT)$, i.e., 3.3, by comparison to those of the d(G•C) pairs, and that the stabilities of the d(A•T) and r(A•U) pairs are comparable.

The proton exchange experiments, which show that the r(G•C) apparent dissociation constants are about two times smaller than that of the d(G•C) pairs, and that the stability of the d(A•T) and r(A•U) pairs are comparable, correlate fairly well with the thermodynamic properties derived from the comparison of the DNA and RNA melting temperatures. Nevertheless, the processes are different, so correlation may be in part coincidental.

ACKNOWLEDGMENT

We thank Maurice Guéron for continuing interest and stimulating discussions during this study. Sylvie Nonin-Lecomte is gratefully acknowledged for comments on the manuscript.

REFERENCES

1. Guéron, M., and Leroy, J.-L. (1995) *Methods Enzymol.* 261, 383–413.
2. Nonin, S., Leroy, J.-L., and Guéron, M. (1995) *Biochemistry* 34, 10652–59.
3. Leroy, J.-L., Kochoyan, M., Huynh-Dinh, T., and Guéron, M. (1988) *J. Mol. Biol.* 200, 223–238.
4. Kochoyan, M., Leroy, J.-L., and Guéron, M. (1987) *J. Mol. Biol.* 196, 599–609.
5. Leroy, J.-L., Charretier, E., Kochoyan, M., and Guéron, M. (1988) *Biochemistry* 27, 8894–8898.
6. Kochoyan, M., Leroy, J.-L., and Guéron, M. (1990) *Biochemistry* 29, 4799–4805.
7. Cain, R. J., and Glick, G. D. (1998) *Biochemistry* 37, 1456–1464.
8. Leijon, M., Sehlstedt, U., Nielsen, P. E., and Graslund, A. (1997) *J. Mol. Biol.* 271, 438–455.
9. Maltseva, T. V., Zarytova, V. F., and Chattopadhyaya, J. (1995) *J. Biochem. Biophys. Methods* 30, 163–177.
10. Leroy, J.-L., Gehring, K., Kettani, A., and Guéron, M. (1993) *Biochemistry* 32, 6019–6031.
11. Wärmländer, S., Sen, A., and Leijon, M. (2000) *Biochemistry* 39, 607–615.
12. Varani, G., Wimberly, B., and Tinoco, I., Jr. (1989) *Biochemistry* 28, 7760–7772.
13. Nonin, S., Jiang, F., and Patel, D. J. (1997) *J. Mol. Biol.* 268, 359–374.
14. Leroy, J.-L., Broseta, D., and Guéron, M. (1985b) *J. Mol. Biol.* 184, 165–78.
15. Leroy, J.-L., Bolo, N., Figueroa, N., Plateau, P., and Guéron, M. (1985) *J. Biomol. Struct. Dyn.* 2, 915–939.
16. Eigen, M. (1964) *Angew. Chem., Int. Ed. Engl.* 3, 1–19.
17. Guéron, M., Charretier, E., Hagerhorst, J., Kochoyan, M., Leroy, J.-L., and Moraillon, A. (1990) in *Structure and Methods, Vol 3: DNA & RNA* (Sarma, R. H., Sarma, M. H., Eds.) pp 113–137, Adenine Press, Guilderland, NY.
18. Guéron, M., Kochoyan, M., and Leroy, J.-L. (1987) *Nature* 382, 89–92.
19. Snoussi, K., Nonin-Lecomte, S., and Leroy, J.-L. (2001) *J. Mol. Biol.* 309, 139–153.
20. Cantor, C. R., Warshaw, M. M., and Shapiro, H. (1970) *Biopolymers* 9, 1059–1077.
21. Morris, G. A., and Freeman, R. (1978) *J. Magn. Res.* 29, 433–462.
22. Phan, A. T., Guéron, M., and Leroy, J.-L. (2001) *Methods Enzymol.* 338, 341–371.
23. Plateau, P., and Guéron, M. (1982) *J. Am. Chem. Soc.* 104, 7310–7311.
24. Guéron, M., and Leroy, J.-L. (1992) in *Nucleic Acids and Molecular Biology*, Vol. 6 (Eckstein, F., Lilley, D. M. J., Eds.) pp 1–22, Springer-Verlag, Berlin.
25. Nonin, S., Leroy, J.-L., and Guéron, M. (1996) *Nucleic Acids Res.* 24, 586–595.
26. Izatt, R. M., Christensen, J. J., and Rytting, J. H. (1971) *Chem. Rev.* 71, 5, 439–480.
27. Auffinger, P., and Westhof, E. (1997) *J. Mol. Biol.* 274, 54–63.
28. Chen, Y. Z., Mohan, V., and Griffey, R. H. (2000) *Phys. Rev. E* 61, 5640–5645.
29. Lesnik, E. A., and Freier, S. M. (1995) *Biochemistry* 34, 10807–10815.
30. Leijon, M., and Leroy, J.-L. (1997) *Biochimie* 79, 775–779.

BI010385D